Understanding the extraordinary magnetoelastic behavior in GdNi

Durga Paudyal,[1] Ya. Mudryk,[1] Y. B. Lee,[1,2] V. K. Pecharsky,[1,3,*] K. A. Gschneidner, Jr.,[1,3] and B. N. Harmon[1,2]
[1]*Ames Laboratory of the USDOE, Iowa State University, Ames, Iowa 50011-3020, USA*
[2]*Department of Physics and Astronomy, Iowa State University, Ames, Iowa 50011-3160, USA*
[3]*Department of Materials Science and Engineering, Iowa State University, Ames, Iowa 50011-2030, USA*
(Received 23 October 2008; published 24 November 2008)

Measurements as a function of both magnetic field and temperature along with first principles spin polarized calculations explain the remarkable magnetoelastic properties exhibited by GdNi below its Curie temperature. The lattice constants a and b elongate continuously by 0.35% and 0.49%, respectively, while the c axis contracts by 0.78%, all without phase volume change. Calculations and experiment confirm a relatively shallow magnetization-dependent energy landscape modified by the increased spin splitting of the conduction band as the $4f$ moments order.

DOI: 10.1103/PhysRevB.78.184436 PACS number(s): 75.80.+q, 61.66.Dk, 71.20.−b

I. INTRODUCTION

Spontaneous magnetoelastic effects in some Gd compounds arise from strain-dependent magnetic exchange interactions which may appear with or without a change in crystallography.[1] For example, pure Gd exhibits an anisotropic magnetostriction below Curie temperature (T_C) and a continuous change in the unit-cell volume but the crystal symmetry remains invariant.[2,3] In other Gd compounds, such as Gd_5T_4 (T=$Si_{1-x}Ge_x$), a structural phase transition accompanied by a discontinuous volume change results in a giant linear magnetostriction [~10 000 parts per million (ppm)], which influences the exchange interactions affecting the magnetic ground state.[4–6] GdNi shows anisotropic shifts in lattice constants exhibiting spontaneous linear magnetostriction effects of 8000 ppm along the c direction and may therefore also be classified as a giant magnetostriction compound.[1,2,7,8] However, as will be shown here, the crystallography of GdNi remains unaltered and the unit-cell volume remains constant across the magnetic ordering transition. Therefore, the mechanism of the magnetostriction in GdNi appears to be different from the two examples mentioned above. In this paper the magnetism of GdNi and its unusual coupling to the crystal structure are described and their electronic origin established.

GdNi crystallizes in the CrB-type structure with the space-group symmetry *Cmcm*. On cooling it undergoes a paramagnetic (PM) to ferromagnetic (FM) transition around 70 K.[9,10] Specific heat of GdNi shows a typical second-order transition at 72 K, which coincides with the Curie temperature.[11–13] The bulk magnetization reported by Abrahams *et al.*[10] indicates that the magnetic moments of Gd align ferromagnetically parallel with the b axis, which is consistent with a nuclear-magnetic-resonance (NMR) study.[14] Paramagnetic GdNi obeys the Curie-Weiss law, and according to several reports its effective moment is ~8.5μ_B, which is larger than 7.94μ_B of the free Gd^{3+} ion.[15,16]

Yano *et al.*[17] claimed an antiferromagnetic (AFM) coupling between the Gd and small Ni moments based on soft x-ray magnetic circular dichroism (XMCD) experiments. A small Gd induced Ni moment is also reported by Mallik and co-workers[15,18,19] from bulk measurements. A local spin-density approximation (LSDA)-based calculation[20] quotes moments of 7.38μ_B for Gd and −0.09μ_B for Ni, affirming a small moment of Ni atoms in GdNi. However, a recent perturbed angular-correlation (PAC) study[21] shows that the hyperfine field vanishes discontinuously indicating a first-order magnetic phase transition in contrast to the second-order behavior deduced from bulk property measurements.[9,10,15] It also indicates no magnetic moments on Ni atoms supporting the earlier report by Ursu and Burzo.[22] The PAC measurements were made using ^{111}Cd nuclei diffusively inserted as radioactive ^{111}In, which may introduce local strains and affect the response of the surrounding lattice.

The brief overview of earlier studies of GdNi given above leaves several important basic questions unanswered. The first question is what effect, if any, the strongly anisotropic strain developing below T_C has on the crystal structure of GdNi. The second is the thermodynamic nature of the magnetic phase transformation, which is still under debate.[2] The third are details of the Gd $5d$–Ni $3d$ hybridization, and finally, the key problem is the mechanism of the remarkably strong linear strain anisotropy in the absence of volume strain. Below we address these questions by coupling experiments with first principles calculations.

II. EXPERIMENTAL DETAILS

The GdNi alloy was prepared by arc melting of the pure metals under argon atmosphere. Gadolinium was obtained from the Materials Preparation Center[23] of the Ames Laboratory (purity of 99.86 at. % with respect to all elements in the Periodic Table including the interstitial elements). Ni (99.88 at. % pure) was purchased from a commercial vendor. One part of the alloy was heat treated at 800 °C for 21 days. The x-ray powder-diffraction study at room temperature was performed using a Bragg-Brentano diffractometer with Cu $K\alpha$ radiation. Low-temperature (5–300 K) x-ray powder-diffraction experiments in various magnetic fields (0–40 kOe) were performed using a Rigaku TTRAX diffractometer with Mo $K\alpha$ radiation.[24] The full profile Rietveld refinement [General Structure Analysis System, GSAS (Ref. 25)] was employed for data analysis. The magnetic properties were measured in a Quantum Design MPMS-XL mag-

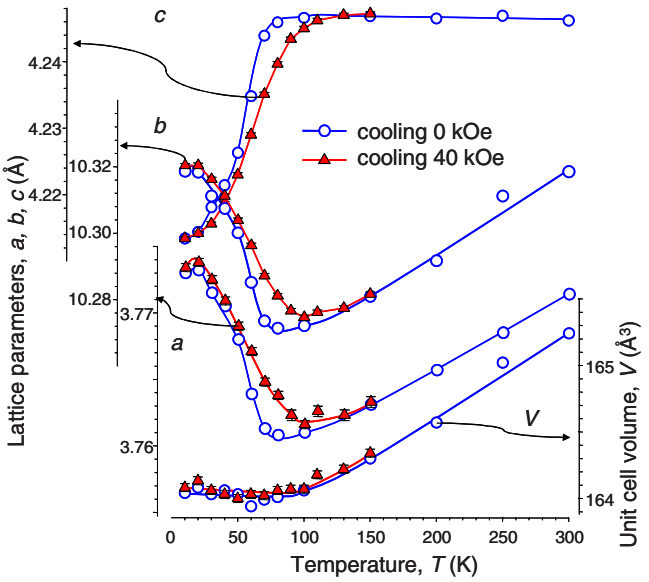

FIG. 1. (Color online) Lattice parameters and unit-cell volume of GdNi as functions of temperature in 0 and 40 kOe magnetic fields.

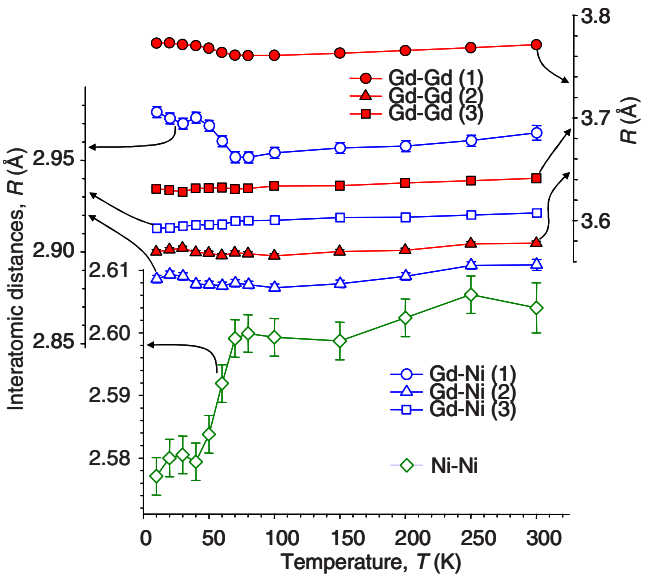

FIG. 2. (Color online) The nearest interatomic distances of GdNi as functions of temperature derived from x-ray powder-diffraction data.

netometer. The heat capacity was measured using an automated heat-pulse calorimeter.[26]

III. RESULTS AND DISCUSSION

A. Experiment

The room-temperature x-ray powder-diffraction patterns of both as cast and heat-treated GdNi alloys can be indexed with the CrB-type structure (space group *Cmcm*). The lattice and atomic parameters at room temperature for the heat-treated sample are $a=3.7713(4)$, $b=10.3272(8)$, and $c=4.2488(3)$ Å; Gd in 4(c): 0, 0.1429(2), $\frac{1}{4}$ and Ni in 4(c): 0, 0.4211(5), $\frac{1}{4}$. Cooling the sample in a zero magnetic field leads to the same thermal-expansion behavior as reported by Lindbaum and co-workers[1,2,7] (Fig. 1). Despite large anisotropic changes in the lattice parameters ($\Delta a/a=0.35\%$, $\Delta b/b=0.49\%$, and $\Delta c/c=-0.78\%$) the structure retains the CrB type at $T=5$ K. The unit-cell volume does not measurably change at and below T_C (Fig. 1).

An analysis of interatomic distances (Fig. 2) shows that below 70 K there is a decrease in Ni-Ni distance and a slight increase in the nearest Gd-Gd and Gd-Ni distances. These changes reflect the anisotropic changes in the unit-cell dimensions and may be correlated with the changes in magnetic states. Indeed, the strong hybridization between Ni $3d$ and Gd $5d$ bands results in changes in the electronic structure (bonding) as the $4f$ moments begin to order. The $4f$-$5d$ (local) exchange increases with magnetization and splits the spin-up and spin-down hybridized states.

Cooling in a 40 kOe magnetic field (Fig. 1) shows a pronounced influence of the magnetic field on the crystal lattice. While the trend of the lattice-parameter change remains the same as in zero field, it is clear that the magnetic field has a strong impact on the values of lattice parameters starting at 90–95 K, well above the T_C of 70 K. In agreement with the temperature dependencies of the lattice parameters in 0 and 40 kOe fields, an isothermal change in the magnetic field leads to a strongly anisotropic linear magnetostriction around the transition temperature, for example, at 60 and 80 K (the latter is shown in Fig. 3). The magnetostriction in a 40 kOe field becomes negligible away from T_C, e.g., at 20 and 100 K (the former is shown in Fig. 3). The magnetostriction of GdNi (~1700 ppm) with 40 kOe field is comparable to that of $La(Fe_{0.88}Co_{0.03}Si_{0.09})_{13}$ (~2000 ppm) with 40 kOe field at $T=240$ K.[27] No change in the unit-cell volume and no sign of an abrupt structural transition with the increasing field were observed.

Magnetization vs temperature measurements performed in $H_{dc}=1$ kOe field (Fig. 4, inset) indicate the FM↔PM transition at $T_C=70$ K. Measurements carried out at $H_{dc}=10$ kOe show a broader transition at the same temperature, determined as the minimum of dM/dT, which is character-

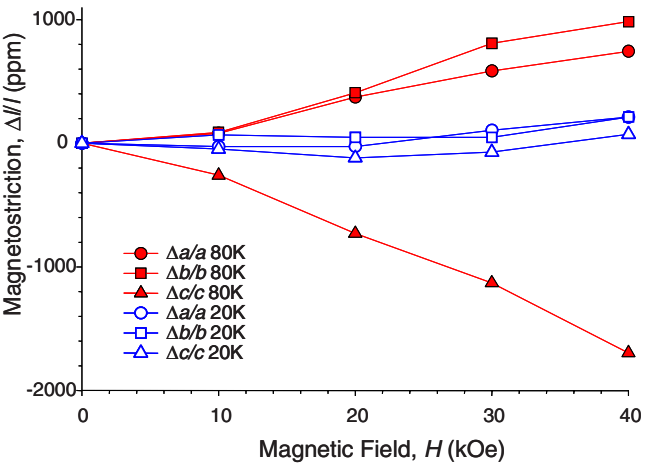

FIG. 3. (Color online) Linear magnetostriction derived from x-ray powder-diffraction data.

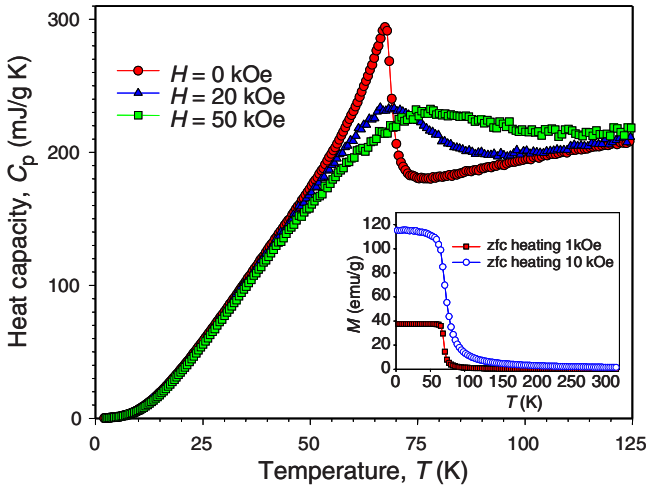

FIG. 4. (Color online) Heat capacity of GdNi as a function of temperature. Inset shows magnetization vs temperature.

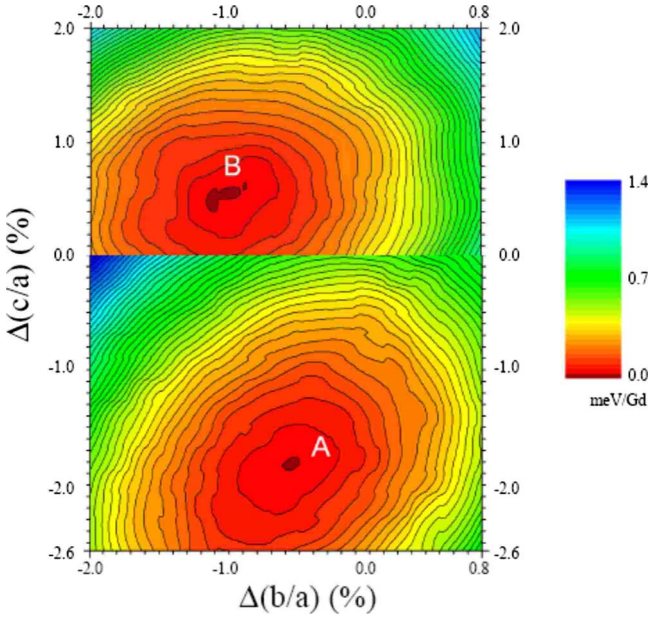

FIG. 5. (Color online) Total energy variation in PM-GdNi (top) and FM-GdNi (bottom) as a function of lattice parameters shown as $\Delta(b/a)$ and $\Delta(c/a)$ for a constant unit-cell volume.

istic for second-order transitions. Above the Curie temperature, the reciprocal susceptibility as a function of temperature is linear up to 320 K, the highest measured point. The Curie-Weiss fit results in θ_p=72.8 K and p_{eff}=8.23μ_B. An analysis of the isothermal magnetization measured at 2 K results in a saturation moment of 7.10(1)μ_B/f.u. which is lower than 7.20μ_B/f.u. calculated from first principles as will be shown below. The saturation moment gradually decreases as the temperature increases. No signs of metamagnetic behavior are observed in the isothermal $M(H)$ data.

The temperature dependence of the heat capacity (Fig. 4) of GdNi in a zero magnetic field shows a lambda-type transition at 70 K, typical for second-order magnetic phase transitions, which correlates well with the magnetic and x-ray measurements. The application of a magnetic field considerably broadens the transition.

B. Theory

In order to gain insight into these unusual experimental phenomena we start with the total energy (E) calculated using experimental data corresponding to the FM structure at 20 K (a=3.774 Å, b=10.320 Å, c=4.215 Å, y/b_{Gd}=0.1397, and y/b_{Ni}=0.4283) and the PM structure at 150 K (a=3.763 Å, b=10.281 Å, c=4.247 Å, y/b_{Gd}=0.1396, and y/b_{Ni}=0.4271) using tight-binding linear muffin-tin orbital method within the atomic sphere approximation (TB-LMTO-ASA).[28] Consistent with the ferromagnetic ground state of GdNi, $E_{\text{FM}}-E_{\text{PM}}$=−2.9 meV/Gd. Here, the PM state was modeled by assigning equal up and down spins in the 4f shell of the Gd ion in order to get zero net 4f moment.

The total-energy calculations described above are within the local spin-density approximation (using the von Barth–Hedin exchange-correlation potentials) with the U correction (Coulomb repulsion between 4f electrons), LSDA+U approach.[29,30] The values of U and J (exchange interaction between localized 4f electrons) are equal to 6.7 and 0.7 eV,[29] respectively. With the lattice constants and atomic positions fixed, the total-energy difference between the magnetic ground state and paramagnetic state is in the range of meV/Gd. To reduce the possible imprecision of the atomic sphere approximation and to consider the full potentials, we have also employed the full potential linear augmented plane-wave (FP-LAPW) method treating 4f electrons as core electrons.

Using FP-LAPW, E_{FM} calculated as a function of lattice parameters, expressed as $\Delta(b/a)$ and $\Delta(c/a)$ keeping unit-cell volume constant, indicates a total-energy minimum (A, Fig. 5) at a=3.8037 Å, b=10.3394 Å, and c=4.1720 Å. The PM calculations show a different minimum (B, Fig. 5) at a=3.7783 Å, b=10.2290 Å, and c=4.2454 Å. We note that the PM and the FM minima are located far apart along the c axis and they are close along the b axis because b and a change in the same direction but c and a change in opposite directions. The calculated total-energy landscape shows no energy barrier between the two minima and is similar to that obtained within the LSDA+U based TB-LMTO approach (not shown) and both minima are close to the experimental lattice parameters (Fig. 1) regardless of the choice of the *ab initio* technique.

Since $E^{\text{A}}_{\text{FM}}-E^{\text{B}}_{\text{FM}}$=−1.5 meV/Gd but $E^{\text{B}}_{\text{PM}}-E^{\text{A}}_{\text{PM}}$=−1.7 meV/Gd, this confirms that the structure with the total-energy minimum in A must be in the FM state and that with the total-energy minimum in B must be in the PM state. Therefore, the highly anisotropic change in the lattice parameters is derived from the change in the magnetic state of GdNi, which rarely happens in real materials unless there is a structural transformation accompanied by a phase volume change. It is interesting to note that considering the magnetic energy $E=-\vec{M}\cdot\vec{B}$, the energy difference (1.62 meV/Gd) between FM-A and PM-B is equivalent to applying a 40 kOe field.

Total energy calculations using both FP-LAPW and LSDA+U based TB-LMTO methods were also performed at

several fixed Gd $4f$ moments at intermediate values between 0 and $7\mu_B$. This simulates the change in the electronic structure with temperature as the magnetism develops below 70 K. We find that the locations of the energy minima change smoothly with magnetization, in agreement with the picture of the increased magnetic alignment of the $4f$ moment (as temperature is lowered below T_C) causing an increased spin splitting of the energy bands, which in turn causes the lattice changes.

The orbital occupation of Gd $5d$ and Ni $3d$ gives rise to $3d$-$5d$ hybridization at the top of the $3d$ band and at the bottom of the $5d$ band. The higher value of the integrated number of electrons up to the Fermi level and orbital projected band centers from LSDA+U TB-LMTO calculations indicate a stronger $5d$-$3d$ hybridization in the FM state than in the PM state, resulting in the FM (T=0 K) ground state of GdNi. The calculations reveal that the band splittings at the Fermi level of Gd $5d$ and Ni $3d$ are 0.58 and −0.05 eV, respectively. Because of this a total of $\sim 0.3\mu_B$ and $\sim -0.1\mu_B$ d moments appear on the Gd and Ni sites. The antiparallel alignment of Gd $5d$ and Ni $3d$ moments is similar to other lanthanide-transition-metal compounds.[31,32] The calculated Ni moment is in excellent agreement with the experimental value ($-0.102\mu_B$) determined from the XMCD measurements.[17]

Figure 6 shows the total density of states (DOS) around the Fermi level corresponding to GdNi in the total-energy minimum A from FP-LAPW calculations. The peak appearing just below the Fermi level (at $\sim$−0.2 eV) in the PM DOS splits into two (spin-up and spin-down) peaks separated by $\sim$0.6 eV around the Fermi level. As the band splitting caused by the magnetism increases, the system simultaneously rearranges its structure by changing the lattice parameters (Fig. 1) and interatomic distances (Fig. 2) to lower the total energy in the FM state. This illustrates that the second-order transformation between B and A is driven smoothly by the magnetism through spin splitting.

IV. CONCLUSIONS

In summary, x-ray diffraction experiments and first principles computations indicate large anisotropic shifts in lattice parameters of GdNi and a giant linear magnetostriction without a first-order structural transition and with a negligible volume magnetostriction. In agreement with the magnetization and heat-capacity experiments, the total-energy and band splitting calculations confirm that the structural changes in GdNi are associated with the second-order FM phase transformation. A small Ni moment antiparallel to the Gd moment is due to the $3d$-$5d$ hybridization occurring at the top of the $3d$ and the bottom of the $5d$ bands. The electronic structure of GdNi leads to an unusual interplay between magnetism and crystal structure, whereas band splitting due to ferromagnetism (ordering of the $4f$ moments) increases, the electronic structure changes continuously causing concomitant anisotropic changes in the lattice to minimize the total free energy of the crystal.

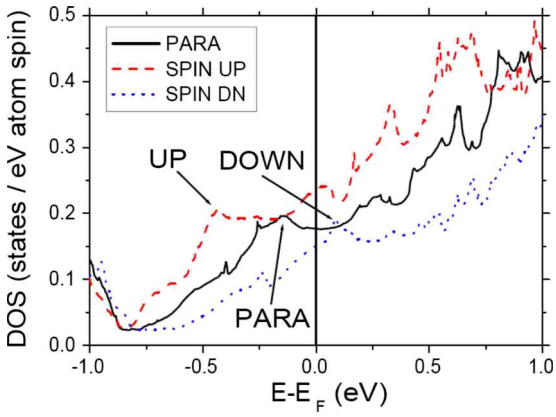

FIG. 6. (Color online) Comparison of PM and FM DOSs of GdNi with lattice parameters corresponding to the FM total-energy minima A.

Note added in proof. Recent heat capacity measurements by Baranov and co-workers,[33] who also observed the second order transition in GdNi at 68 K, are in good agreement with our results.

ACKNOWLEDGMENTS

This work was supported by the Office of Basic Energy Sciences, Materials Sciences Division of the U.S. Department of Energy under Contract No. DE-AC02-07CH11358 with Iowa State University of Science and Technology.

*Corresponding author; vitkp@ameslab.gov

[1] E. Gratz and A. Lindbaum, J. Magn. Magn. Mater. **137**, 115 (1994).
[2] A. Lindbaum and M. Rotter, in *Handbook of Magnetic Materials*, edited by K. H. J. Buschow (Elsevier, New York, 2002), Vol. 14, Chap. 4, p. 307.
[3] F. J. Darnell, Phys. Rev. **130**, 1825 (1963).
[4] V. K. Pecharsky and K. A. Gschneidner, Jr., Pure Appl. Chem. **79**, 1383 (2007).
[5] D. Paudyal, V. K. Pecharsky, K. A. Gschneidner, Jr., and B. N. Harmon, Phys. Rev. B **75**, 094427 (2007).
[6] V. K. Pecharsky, G. D. Samolyuk, V. P. Antropov, A. O. Pecharsky, and K. A. Gschneidner, Jr., J. Solid State Chem. **171**, 57 (2003).
[7] E. Gratz and A. Lindbaum, J. Magn. Magn. Mater. **177-181**, 1077 (1998).
[8] K. Uhlířová, J. Prokleška, J. Poltierová Vejpravová, V. Sechovský, and K. Maezawa, J. Magn. Magn. Mater. **310**, 1753 (2007).
[9] R. E. Walline and W. E. Wallace, J. Chem. Phys. **41**, 1587 (1964).
[10] S. C. Abrahams, J. L. Bernstein, R. C. Sherwood, J. H. Wernick, and H. J. Williams, J. Phys. Chem. Solids **25**, 1069 (1964).
[11] K. Sato, Y. Isikawa, K. Mori, and T. Miyazaki, J. Appl. Phys. **67**,

5300 (1990).
[12] C. B. Zimm, W. F. Stewart, J. A. Barclay, W. Overton, C. Olsen, D. Harding, R. Chesebrough, and W. Johanson, Adv. Cryog. Eng. **33**, 791 (1988).
[13] J. A. Blanco, J. C. Gomez Sal, J. Rodriguez Fernandez, M. Castro, R. Burriel, D. Gignoux, and D. Schmitt, Solid State Commun. **89**, 389 (1994).
[14] V. L. B. de Jesus, V. M. T. S. Barthem, I. S. Oliveira, and A. P. Guimarães, J. Magn. Magn. Mater. **177-181**, 1125 (1998).
[15] R. Mallik, P. L. Paulose, E. V. Sampathkumaran, S. Patil, and V. Nagarajan, Phys. Rev. B **55**, 8369 (1997).
[16] J. A. Blanco, J. C. Gomez Sal, J. Rodriguez Fernandez, D. Gignoux, D. Schmitt, and J. Rodriguez-Carvajal, J. Phys.: Condens. Matter **4**, 8233 (1992).
[17] K. Yano, I. Umehara, K. Sato, and A. Yaresko, Solid State Commun. **136**, 67 (2005).
[18] R. Mallik, E. V. Sampathkumaran, P. L. Paulose, and V. Nagarajan, Phys. Rev. B **55**, R8650 (1997).
[19] P. L. Paulose, S. Patil, R. Mallik, E. V. Sampathkumaran, and V. Nagarajan, Physica B **223-224**, 382 (1996).
[20] J. Rusz, I. Turek, and M. Diviŝ, Phys. Rev. B **71**, 174408 (2005).
[21] P. de La Presa and M. Forker, Hyperfine Interact. **158**, 261 (2004).
[22] I. Ursu and E. Burzo, J. Magn. Reson. (1969-1992) **8**, 274 (1972).
[23] Materials Preparation Center, Ames Laboratory of U.S. DOE, Ames, IA, USA (www.mpc.ameslab.gov).
[24] A. P. Holm, V. K. Pecharsky, K. A. Gschneidner, Jr., R. Rink, and M. Jirmanus, Rev. Sci. Instrum. **75**, 1081 (2004).
[25] B. H. Toby, J. Appl. Crystallogr. **34**, 210 (2001); A. C. Larson and R. B. von Dreele, Los Alamos National Laboratory Report No. LAUR 86-748, 1986 (unpublished).
[26] V. K. Pecharsky, J. O. Moorman, and K. A. Gschneidner, Jr., Rev. Sci. Instrum. **68**, 4196 (1997).
[27] A. Fujita and K. Fukamichi, IEEE Trans. Magn. **35**, 3796 (1999).
[28] O. K. Andersen and O. Jepsen, Phys. Rev. Lett. **53**, 2571 (1984).
[29] V. I. Anisimov, F. Aryasetiawan, and A. I. Lichtenstein, J. Phys.: Condens. Matter **9**, 767 (1997).
[30] B. N. Harmon, V. P. Antropov, A. I. Liechtenstein, I. V. Solovyev, and V. I. Anisimov, J. Phys. Chem. Solids **56**, 1521 (1995).
[31] I. A. Campbell, J. Phys. F: Met. Phys. **2**, L47 (1972).
[32] N. H. Duc, in *Handbook on the Physics and Chemistry of Rare Earths*, edited by K. A. Gschneidner, Jr. and L. R. Eyring (Elsevier Science, New York/North-Holland, Amsterdam, 1997), Vol. 24, p. 339.
[33] N. V. Baranov, H. Michor, G. Hilscher, A. Proshkin, and A. Podlesnyak, J. Phys.: Condens. Matter **20**, 325233 (2008).